GEOPHYSICS, VOL. 47, NO. 1 (JANUARY 1982); P. 100–116, 21 FIGS.

GL04074

Controlled-source audiomagnetotellurics in geothermal exploration

Stewart K. Sandberg* and Gerald W. Hohmann‡

ABSTRACT

Theoretical and field tests indicate that the controlled-source audiomagnetotelluric (CSAMT) method provides an efficient means of delineating the shallow resistivity pattern above a hydrothermal system. Utilizing a transmitter overcomes the main limitation of conventional audiomagnetotelluries—variable and unreliable natural source fields. Reliable CSAMT measurements can be made with a simple scalar receiver. Our calculations for a half-space show that the plane-wave assumption is valid when the transmitter is more than 3 skin depths away in the broadside configuration and more than 5 skin depths away in the collinear configuration. Three dimensional (3-D) numerical modeling results for a bipole source 5 skin depths away compare well with those for a plane-wave source, showing that the method is valid.

A CSAMT survey at the Roosevelt Hot Springs geothermal area in Utah produced apparent resistivity contour maps at four frequencies: 32, 98, 977, and 5208 Hz. These maps show the same features as those of a dipole dipole resistivity map. We also collected detailed CSAMT data at 10 frequencies on two profiles. Two-dimensional (2-D) plane wave modeling (transverse magnetic mode) of the resulting pseudo-sections yields models similar to those derived by modeling the dipole-dipole resistivity data. However, CSAMT resolved details not shown by the resistivity modeling. Thus, high resolution along with an efficient field procedure make CSAMT an attractive tool for geothermal exploration.

INTRODUCTION

Dipole-dipole resistivity and scalar audiomagnetotelluric (AMT) surveys frequently are conducted to delineate the shallow resistivity pattern above a hydrothermal system. The former method is slow and expensive, while the latter is not dependable. Natural fields in the AMT band (10–10^4 Hz) are due to thunderstorm energy propagating in the earth-ionosphere cavity; therefore, the source fields at certain times of the day or in certain seasons may be so weak that it is impossible to obtain reliable data. Furthermore, tensor measurements are required, because the source field direction varies with time. These limitations can be overcome by utilizing a controlled source, i.e., a grounded wire driven at one or several frequencies and located far enough away that the incident field at the receiver approximates a plane wave.

Strangway et al (1973) discussed the application of natural-field AMT in mineral exploration. Hoover et al (1976), Hoover and Long (1976), Hoover et al (1978), and Long and Kaufman (1980) described reconnaissance natural-field AMT investigations with station spacings of several kilometers in geothermal areas. However, in geothermal exploration AMT may be most useful for detailed mapping of near-surface low resistivity zones due to rock alteration and saline pore fluids.

Goldstein and Strangway (1975) introduced the use of a controlled source for AMT surveys and discussed applications in mineral exploration. If the source is located several skin depths from the observation point, the electromagnetic (EM) field behaves as a plane wave, and the conventional magnetotelluric (MT) formula for apparent resistivity can be used to reduce the data.

We investigate the validity of the plane-wave approximation for half-space and three-dimensional (3-D) models. Then we describe the results and interpretation of a controlled source audiomagnetotelluric (CSAMT) survey at the Roosevelt Hot Springs KGRA (known geothermal resource area) in Utah.

PLANE-WAVE APPROXIMATION

Expressions for the magnetic and electric fields due to an infinitesimal grounded electric dipole on a half-space were presented by Goldstein and Strangway (1975). We integrated the infinitesimal dipole solution numerically over a finite length source to simulate a field situation. Solutions were calculated over a 3¼ × 3¼ mile (5.23 × 5.23 km) grid for a 2000 ft (609.6 m) transmitter, a half-space resistivity of 100 Ω·m, and a frequency of 32.02 Hz.

AMT scalar apparent resistivities are calculated according to the relation

$$\rho_a = \frac{1}{\mu\omega}\,\frac{|E|^2}{|H|^2},$$

where E and H are perpendicular horizontal electric and magnetic field components, respectively. For our half-space model, the transmitter bipole is oriented along the x axis.

Figure 1 shows apparent resistivities calculated using the component of the electric field parallel to the transmitter. For

Presented at the 50th Annual International SEG Meeting, November 18, 1980 in Houston. Manuscript received by the Editor September 2, 1980; revised manuscript received April 30, 1981.
*Amoco Minerals Co., 333 West Hampden, Englewood, CO 80110.
‡Dept. of Geology and Geophysics, University of Utah, Salt Lake City, UT 84112.

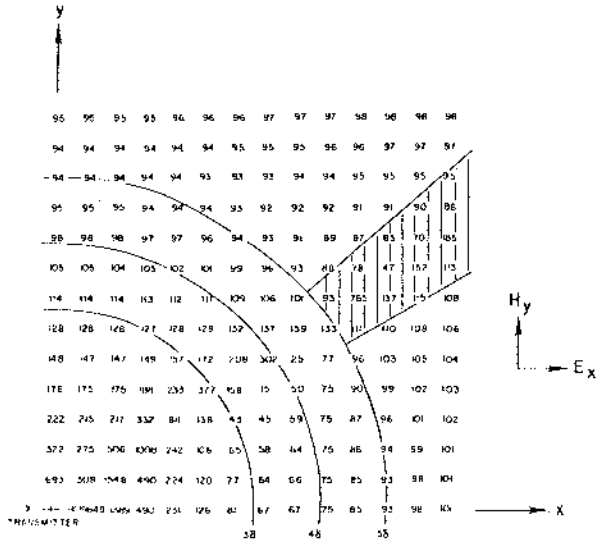

FIG. 1. Apparent resistivities calculated using E_x and H_y with the transmitter bipole parallel to the x-axis. Station spacing 1/4 mi (402.34 m), transmitter bipole 2000 ft (609.6 m) long, half-space resistivity = 100 Ω-m, frequency = 32.02 Hz, skin depth (δ) = 884 m (.55 mi). Three, four, and five skin depth distances from the center of the transmitter are shown. The shaded area is the region of minimum coupling.

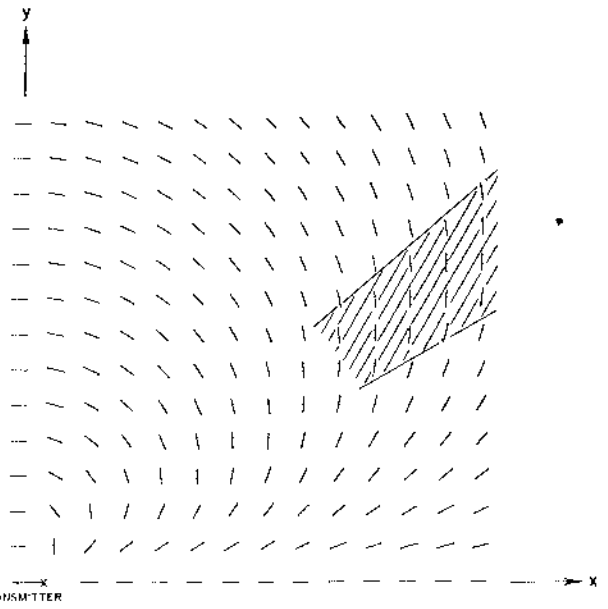

FIG. 2. Orientations of the major axes of the electric field polarization ellipses. The shaded area is the same as that in Figure 1.

reference, distances of 3, 4, and 5 skin depths ($\delta = \sqrt{2/\mu\omega\sigma}$) are shown. Apparent resistivities are within ten percent of the true half-space resistivity (100 Ω-m) when measured more than three skin depths broadside to the transmitter, and more than five skin depths collinear with the transmitter. The broadside configuration refers to measuring the electric field parallel to the transmitter bipole and on its center line. Collinear refers to measuring the electric field parallel to the transmitter bipole and on its axis. However, resistivities in the shaded region of Figure 1, although far enough away, are not within ten percent of 100 Ω-m because the electric and magnetic fields are almost perpendicular to the measuring directions.

Orientations of the major axes of the electric and magnetic field polarization ellipses are plotted in plan view in Figures 2 and 3, respectively. The shaded areas in these figures correspond to the minimum coupling area in Figure 1. Note that in the shaded areas E_x and H_y (the field components used in the apparent resistivity calculations of Figure 1) are small. Apparent resistivities calculated using these small inaccurate components are erratic; the same would be true of field data. Goldstein and Strangway (1975) showed similar regions of minimum coupling on apparent resistivity grids from an infinitesimal electric dipole source.

Figure 4 shows apparent resistivities calculated using the component of the electric field perpendicular to the transmitter bipole. At distances from the transmitter greater than three skin depths, calculated apparent resistivities are everywhere within ten percent of the true half-space resistivity. Minimum coupling in this orientation occurs along the x- and y-axes; no apparent resistivity values are shown on the axes because the E_y and H_x fields are zero.

Profiling parallel to the transmitter bipole (broadside configuration) requires measuring electric and magnetic fields in directions which are not maximum coupling orientations. A profile along a radial path perpendicular to or collinear with the bipole will preserve maximum coupling along the entire profile, and it is therefore recommended.

Kan and Clay (1979) showed half-space solutions for the fields within the earth using a dipole transmitter and stated that the plane-wave source approximation is valid beyond about six skin depths. Their results are based on phases of the fields in the earth.

Three-dimensional (3-D) modeling was employed to simulate the CSAMT technique in the general case and to check the plane-wave approximation for an inhomogeneity in a half-space. The program modeled a bipole source on a 3-D earth using an integral equation solution (Hohmann, 1975). A similar program (Ting and Hohmann, 1981) simulated a plane-wave source over the same 3-D earth for comparison. The 3-D earth consisted of a homogeneous half-space in which a conductive rectangular prism 300 × 600 × 50 m thick was buried 50 m deep. The frequency was 100 Hz, the half-space resistivity was 100 Ω-m, and the prism resistivity was 10 Ω-m.

The first source was located approximately five skin depths from the body, representing a transmitter-receiver separation adequate for the broadside configuration and just large enough for the collinear configuration. Figure 5a shows a plan map of apparent resistivities calculated on profiles across the buried prism using E_y and H_x with transmitter electrodes located 2600 and 3200 m from the origin on the y-axis. The nearest source electrode is 4.9 skin depths from the nearest edge of the body, and the geometry corresponds to the collinear configuration.

In Figure 5b, apparent resistivities are calculated in the same manner, except the source is a plane wave with the electric field polarization in the y-direction. A comparison of Figures 5a and 5b shows the validity of the plane wave approximation for an inhomogeneous earth. Discrepancies are larger on the source side of the body because it is closer to the transmitter bipole.

Figure 6a shows apparent resistivities calculated from E_x and

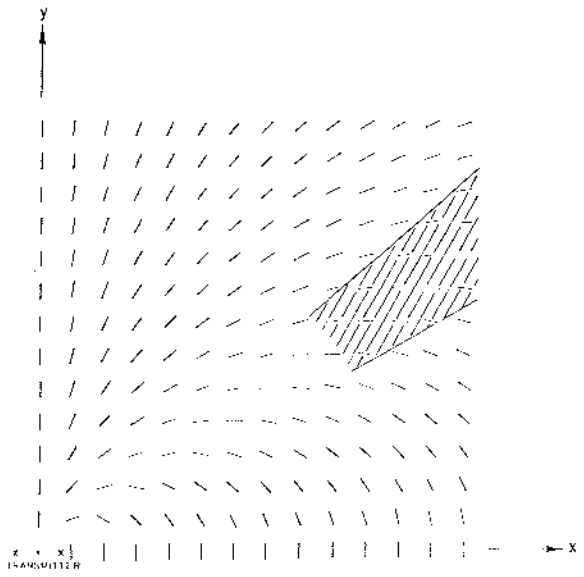

FIG. 3. Orientations of the major axes of the magnetic field polarization ellipses. The shaded area is the same as that in Figure 1.

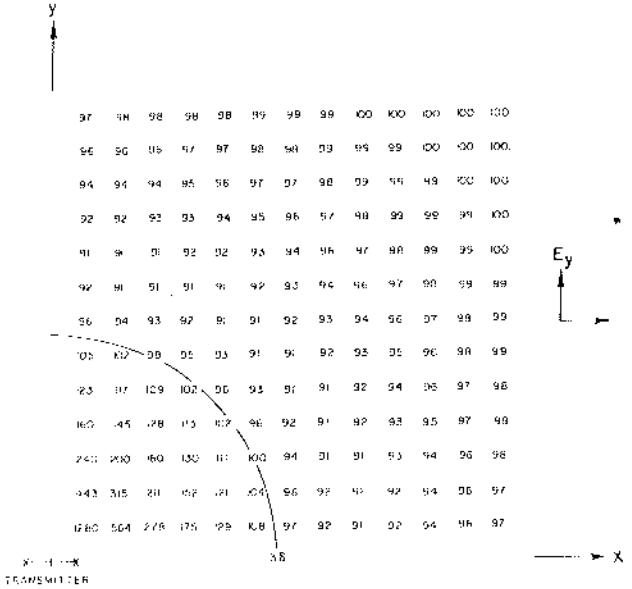

FIG. 4. Apparent resistivities calculated using E_y and H_x with the transmitter bipole parallel to the x-axis. Three skin depths distance from the center of the transmitter is shown.

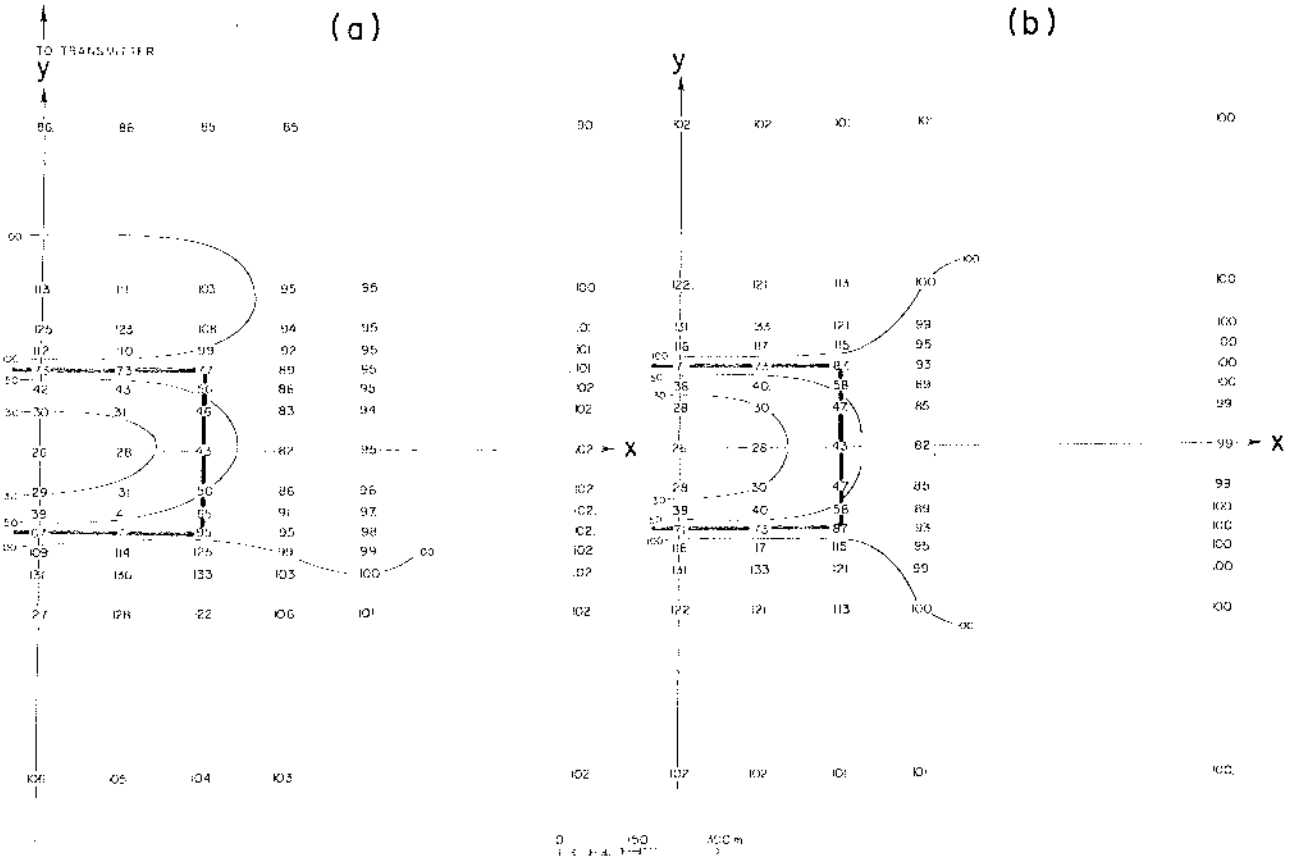

FIG. 5. Plan view of apparent resistivities over a buried 3-D prism calculated using E_x and H_y. Due to the symmetry, only half of the area is shown. Prism resistivity = 10 Ω m, background half space resistivity = 100 Ω m, frequency = 100 Hz. (a) Transmitter bipole in collinear configuration centered at y = 2900 m. (b) Plane-wave source with the electric field polarized in the y direction. A profile of data along y = 600 m has been added in (a) to constrain the apparent resistivity contours.

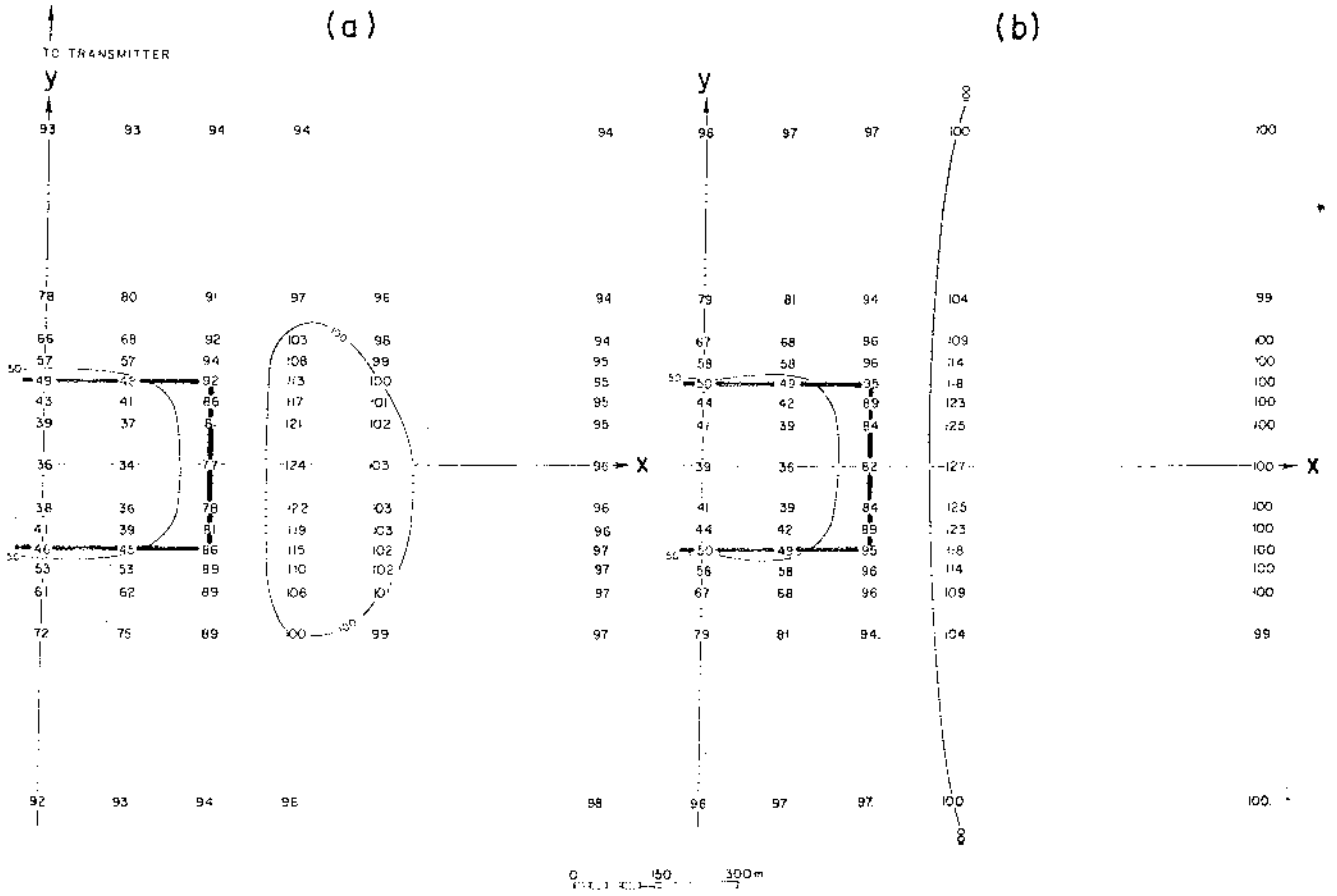

FIG. 6. Plan view of apparent resistivities over a buried 3-D prism calculated using E_x and H_y. (a) Transmitter bipole in broadside configuration centered at $y = 2900$ m. (b) Plane-wave source with the electric field polarized in the y-direction. A profile of data along $y = 600$ m has been added in (a) to constrain the apparent resistivity contours.

H_y for transmitter electrodes centered 2900 m from the origin in the y-direction (5.8 skin depths from the center of the prism) and parallel to the x-axis, i.e., the broadside configuration. For comparison, Figure 6b shows apparent resistivities for a plane-wave source with the electric field in the x-direction. There is good agreement, showing that the source is sufficiently far away that the plane-wave approximation is valid.

The effect of obtaining data too close to the transmitter was simulated by placing source electrodes on the y-axis 700 and 1300 m from the origin in Figure 7a. Electrodes 900 m from the origin in the y-direction and parallel to the x-axis represent the other incident field mode in Figure 7b. Both modes exhibit resistivity lows over the buried prism, but the apparent resistivities are far from the plane-wave values shown in Figures 5b and 6b. The incident field does not approximate a plane wave in this case, because the distance from the center of the transmitter to the center of the body is only 1.8 skin depths.

When applying CSAMT in highly resistive terrain, the required transmitter-receiver separation may be so large that obtaining data too close to the transmitter is necessary in order to receive the signal. Such data are not quantitatively interpretable with plane-wave MT modeling. Goldstein and Strangway (1975) presented curves for one-dimensional (1-D) interpretation of soundings taken too close to the transmitter.

ROOSEVELT HOT SPRINGS CSAMT SURVEY

We carried out a CSAMT survey at Roosevelt Hot Springs KGRA during August and September, 1979. The KGRA is located in Beaver County, in west central Utah on the western margin of the Mineral Mountains. Bedrock in the area is dominated by metamorphic rocks of Precambrian and Paleozoic age. The geothermal system is located within the granitic Mineral Mountains pluton of Tertiary age. There is evidence of recent igneous activity in rhyolite flows, domes, and pyroclastics of Pleistocene age.

The area has been studied in detail by the Dept. of Geology and Geophysics, University of Utah and by the Earth Science Laboratory, University of Utah Research Institute. A summary of the work can be found in Ward et al (1978). Because the area is so well documented, it is a good location for testing an exploration technique.

Roosevelt Hot Springs is a structurally controlled geothermal reservoir. Geothermal exploration targets are the faults and fractures which control the movement of fluids. Alteration products observed along these faults and fractures are associated with chemical reactions caused by the hydrothermal system. Due to the alteration minerals and the brine, the fault zones respond as low-resistivity anomalies in an otherwise moderate to high-resistivity background.

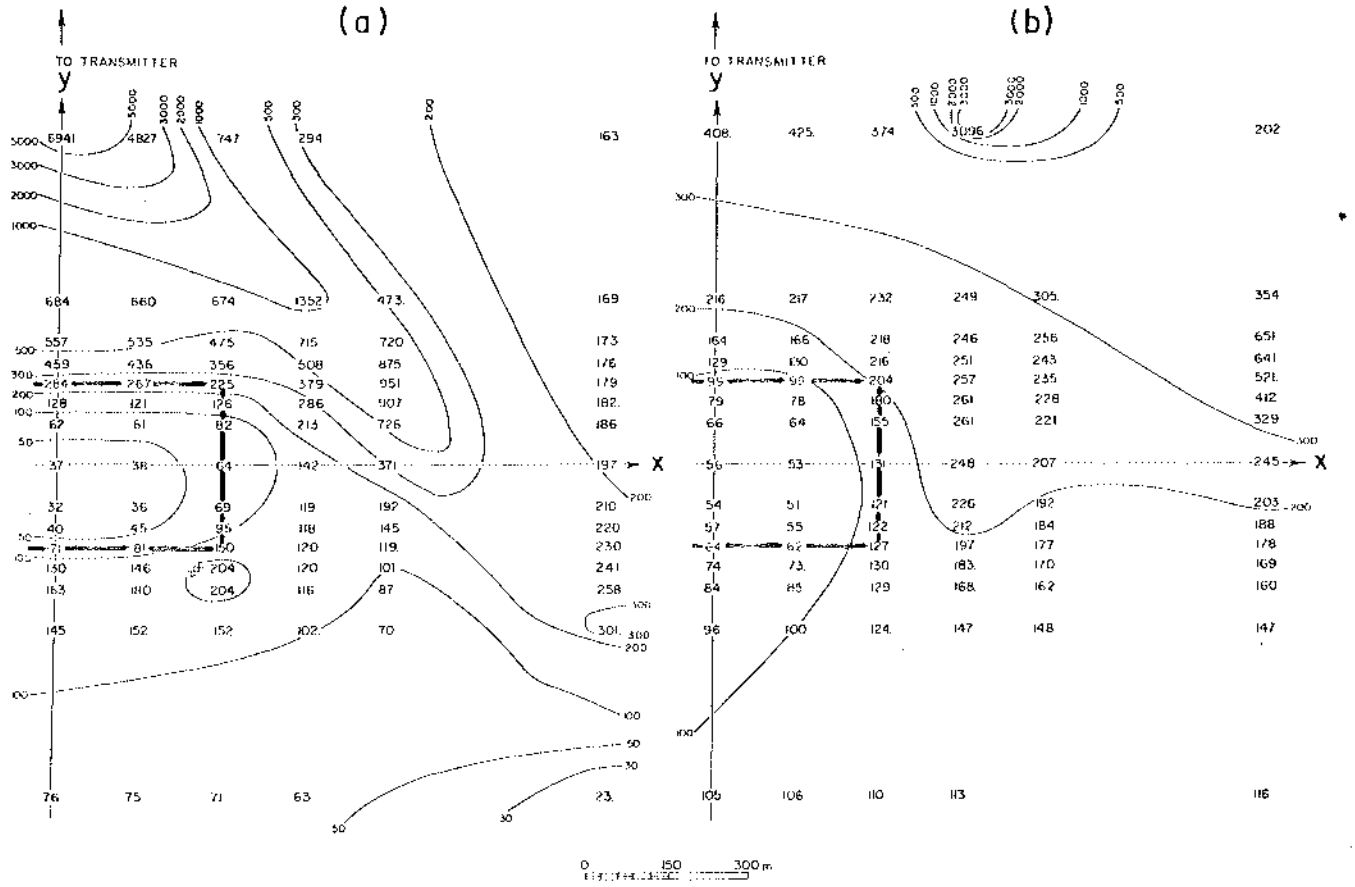

FIG. 7. (a) Same as Figure 5a except transmitter is centered at $y = 1000$ m. (b) Same as Figure 6a except transmitter is centered at $y = 900$ m.

The resistivity range expected is between one and a few hundred ohm-meters. Formation water resistivities are in the range 0.5 to 2 Ω-m (Glenn and Hulen, 1979). Laboratory measurements on core samples from the clay alteration zone (30–60 m) in drillhole 1A near the Opal Mound fault show resistivities as low as 3–5 Ω-m (Ward and Sill, 1976).

Previous resistivity work was done in the area by Ward and Sill (1976). A first separation ($n = 1$) 300-m dipole-dipole resistivity contour map from their work is shown in Figure 8. They used this map (along with dipole-dipole resistivity pseudo sections, an aeromagnetic map, air photos, plus mapped and interpreted geology) to produce a fracture map of the Roosevelt Hot Springs KGRA. Resistivity contours were also used to support the possibility that brine is leaking out of the convective hydrothermal system to the north.

We carried out the CSAMT survey in two parts. First, a resistivity mapping study was completed to assess the method by comparing it with the dipole-dipole resistivity map (Figure 8). The second part of the survey consisted of two east-west profiles across the low-resistivity zone, with subsequent quantitative interpretation using a 2-D MT modeling program.

The transmitter used in the field work was a Geotronics model EMT-5000. The receiver was a Kennecott Minerals Co. scalar AMT unit consisting of a two-channel, tunable, high-gain, narrow band-pass analog instrument which measured the logarithmic ratio of the channel inputs. A reading consisted of an electric-to-magnetic field ratio with no phase information.

The depth of exploration usually given for AMT is one skin depth. However, actual depth of exploration is somewhat less, as discussed later in this paper. In our field work, the lowest frequency was 32 Hz, so in 10 Ω-m ground the depth of exploration is less than 280 m, while in 50 Ω-m ground, it is less than 628 m.

Resistivity mapping

The CSAMT procedure for resistivity mapping is based on our theoretical results. The assumption of a 1-D (layered) earth at each receiver site allows apparent resistivity calculations to be made by measuring the field in maximum coupling orientations. A transparent plot of electric field direction (Figure 2) over a half-space is constructed at the same scale as the field map. Overlaying the field direction plot helps to orient the receiver for maximum signal strength. The distance from the transmitter should be at least three skin depths, using the largest resistivity between receiver and transmitter and the lowest frequency of the sounding. Apparent resistivities are calculated for several frequencies at each station, and a contour map is constructed for each frequency to delineate the near-surface resistivity pattern.

Field work at Roosevelt Hot Springs KGRA resulted in 136 unique stations occupied, 47 of which were located on two pro

files. For resistivity mapping, apparent resistivities were measured at four frequencies: 5208, 977, 98, and 32 Hz. Two transmitter sites were used for the reconnaissance survey, and three others were occupied for profiling. Apparent resistivity contour maps at each of the four frequencies are shown in Figures 9, 10, 11, and 12. The general contour trend and the positions of the low-resistivity zones compare well with the first separation dipole-dipole resistivity map in Figure 8.

The 5208 Hz map of Figure 9 exhibits two zones of low apparent resistivity. One is located around the early steam well. The other is just west of well 3-1 and trends northwest from there through well 82-33 and northeast toward well 12-35. The low resistivities coincide with mapped near-surface alteration and brines associated with the geothermal system. These low resistivities are bounded on the east by the more resistive unaltered granitic pluton, and on the west by unaltered alluvium west of the Opal Mound. Geothermal production wells lie within or just to the east of the low-resistivity zone, and nonproducing wells lie to the south and west. The 100 Ω-m contour north of well 82-33 is not due to noise in the data; high resistivities also occur here in 100-m dipole-dipole data.

The 977 Hz map of Figure 10 defines the same general resistivity trend. A station in the northwest part of the map has a low apparent resistivity of 15 Ω-m. This low-resistivity area

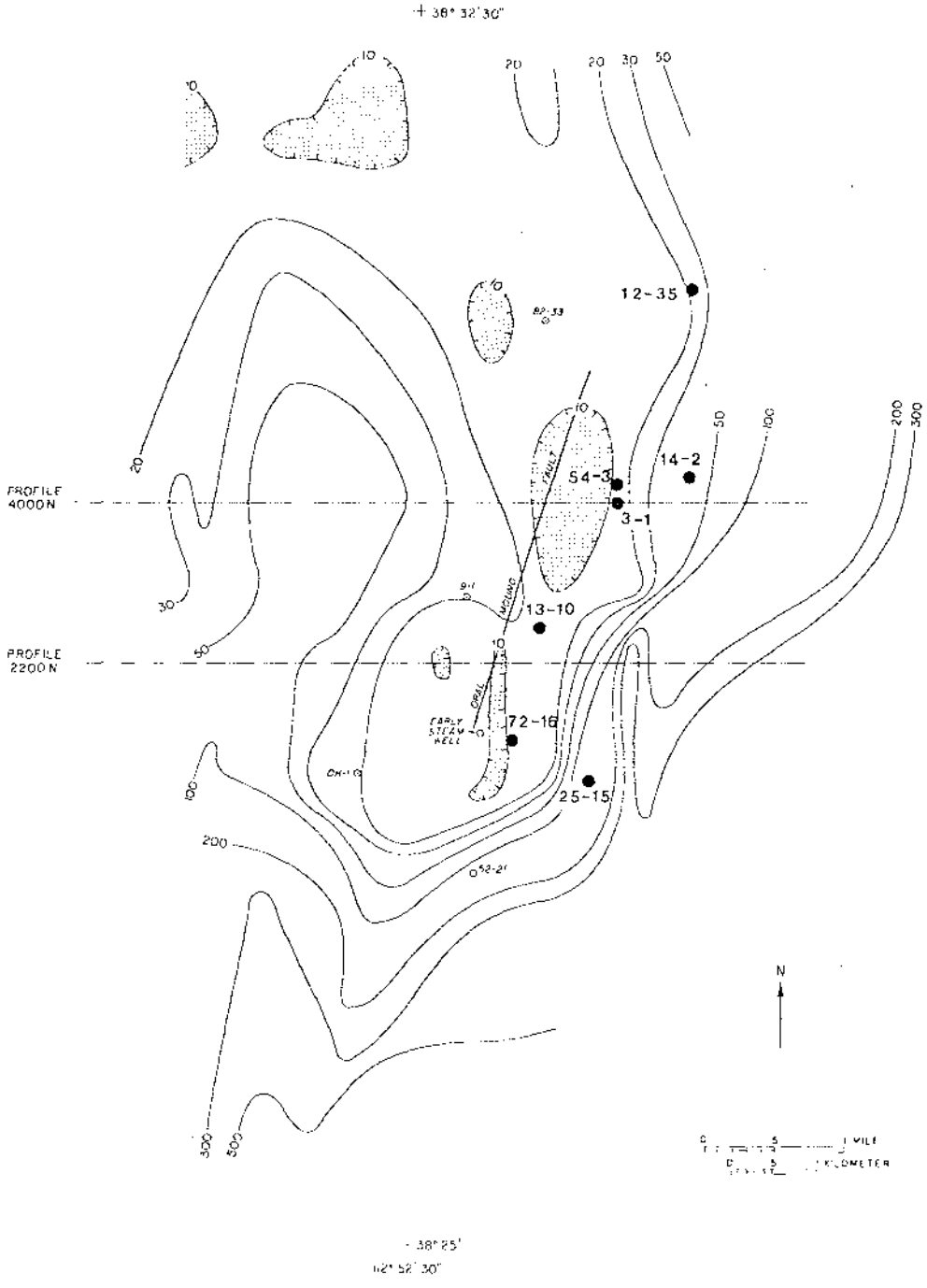

FIG. 8. First separation dipole-dipole resistivity map of the Roosevelt Hot Springs KGRA (a = 300 m). After Ward and Sill (1976). Areas less than 10 Ω-m are shaded. Solid circles denote producing geothermal wells, open circles indicate nonproducing wells.

broadens and becomes more defined in the maps of apparent resistivity for the lower frequencies. Prehistoric Lake Bonneville sediments in this area (Ward and Sill, 1976) explain the feature. The northern low-resistivity zone along the Opal Mound fault extends farther northwest at this frequency. This could indicate that the geothermal system is leaking or has leaked to the northwest.

The 97.7 Hz map of Figure 11 shows low resistivity zones larger in area, with the northern zone extending due north. The conductive zone to the northwest is well defined.

The 32.02 Hz map of Figure 12 shows bedrock to the east and southeast indicated by the high apparent resistivity values. Conductive zones correspond to the geothermal areas as well as the Lake Bonneville sediments to the northwest. The conductive zone along 2200N at the Opal Mound fault is enlarged to the west at this frequency, possibly indicating westward brine leakage from the fault.

The absolute accuracy of the resistivities obtained by our equipment was checked by reoccupying an MT site obtained in an earlier survey. CSAMT data agree with the MT data within measurement error, indicating that our equipment was working properly and apparent resistivities are accurate.

In order to determine the reliability of the data obtained in the survey, we repeated several stations. The repeatability was usually within one decibel of the E/H ratio read from the receiver (one decibel greater corresponds to multiplying the apparent resistivity by 1.26, and one decibel less yields apparent resistivity divided by 1.26). Two receiver and coil sets were used; ratio differences

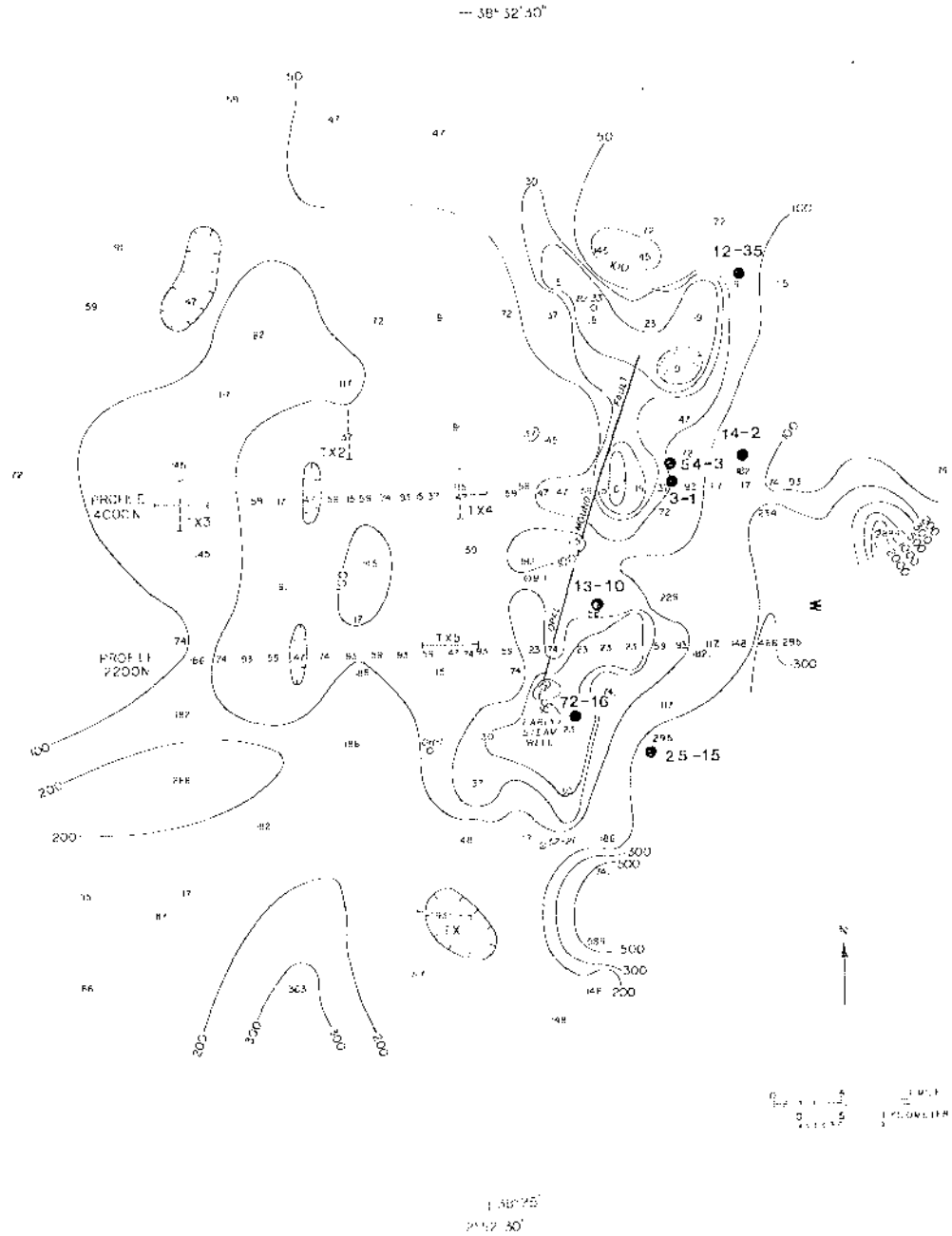

FIG. 9. CSAMT apparent resistivity map of Roosevelt Hot Springs KGRA. Frequency = 5208 Hz. Areas less than 10 Ω-m are shaded.

between the two different sets usually were within one decibel of each other. These accuracy and repeatability tests are explained in more detail in Sandberg (1980).

A CSAMT resistivity mapping survey appears to be more efficient than conventional dipole-dipole resistivity mapping. The CSAMT receiver only requires a 30 m wire for the electric field sensor and a portable coil for detecting the magnetic field, instead of several hundred meters of wire as in the dipole-dipole resistivity procedure. We found that a four-frequency CSAMT station could be read in about 15 minutes, including set-up. Also, since the technique does not need to be confined to profiles, as in the case of dipole-dipole resistivity, rapid areal coverage is possible using existing roads.

The similarity between the CSAMT maps and the first separation dipole-dipole resistivity map, along with the reoccupied MT site results and repeatability tests, indicate that these data are accurate enough for quantitative interpretation. We ran two profiles across the low-resistivity zone and modeled the results. The locations of the profiles are shown in Figure 9.

Profile 1

Profile 1 is an east-west traverse along dipole-dipole resistivity line 4000N (Figure 8). The CSAMT station spacing was 300 m, and two transmitter locations (labeled TX3 and TX4 in Figure 9) were used. The transmitter consisted of an orthogonal pair of 2000 ft (609.6 m) bipoles, allowing apparent resistivity measure-

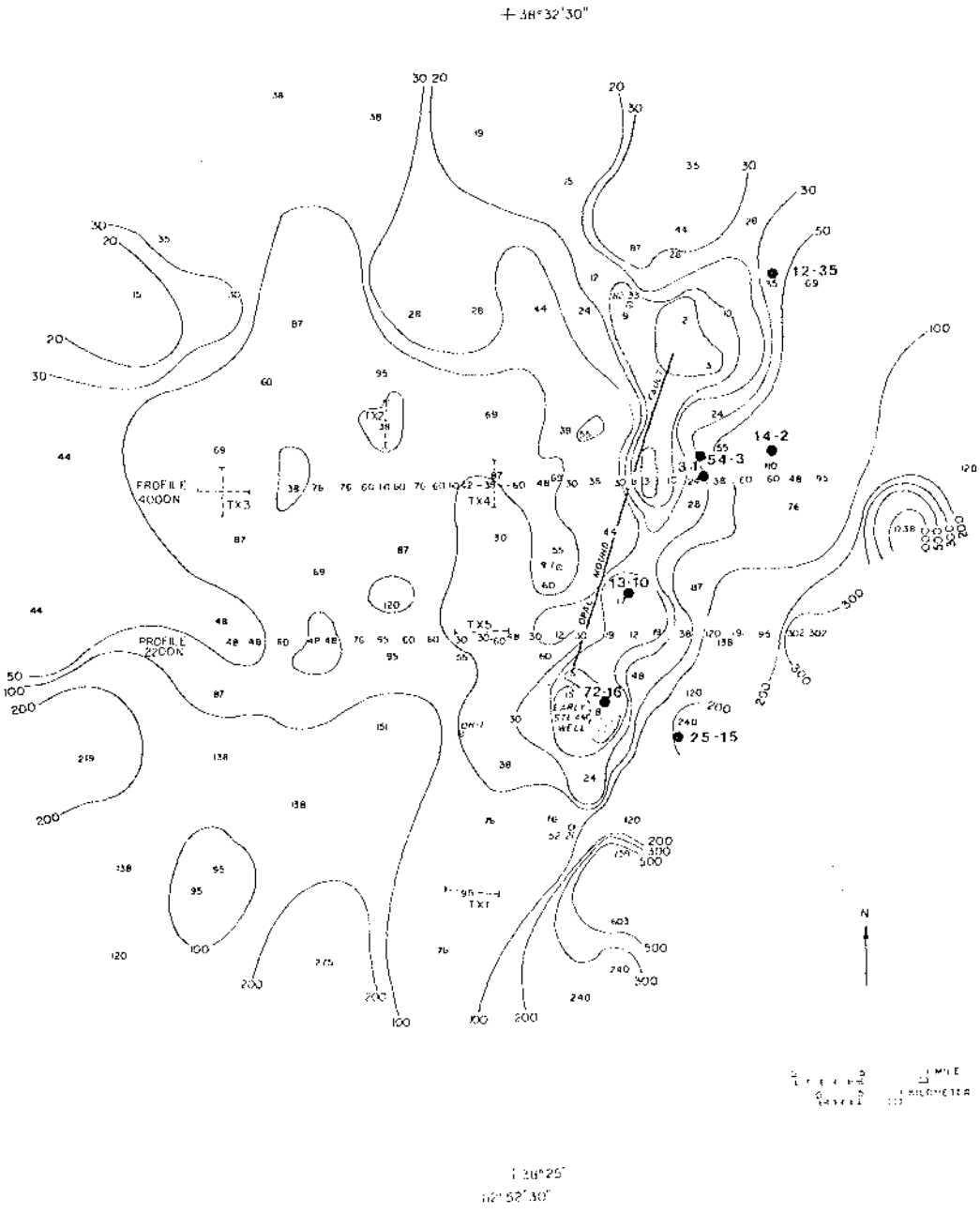

FIG. 10. CSAMT apparent resistivity map of Roosevelt Hot Springs KGRA. Frequency = 977 Hz. Areas less than 10 Ω-m are shaded.

ments with the electric field perpendicular and parallel to the traverse. Two sets of data were thereby obtained, corresponding to electric field orientations perpendicular (TM) and parallel (TE) to geologic strike. The two sets of data are plotted as pseudo-sections in Figures 13 and 14.

One-dimensional MT inversion of the TM mode data at each station along the profile resulted in an initial 2-D resistivity model for the line. This model was then refined by utilizing a 2-D MT finite-element forward computer program (Stodt, 1978) and adjusting the model to fit the TM mode field data. In a complex area such as this, 2-D interpretation is possible only for TM mode data (Wannamaker et al, 1980). The resulting model is shown in Figure 15 along with a 2-D resistivity model for the same line (Ross et al, 1981) derived from combined 100- and 300-m dipole-dipole ($n \leq 4$) data (Ward and Sill, 1976). Theoretical AMT pseudo-sections for the CSAMT and resistivity models are shown in Figures 16 and 17, respectively. These theoretical pseudo-sections can be compared with the field data in Figure 13. The resistivity model AMT response (Figure 17) does not fit the low-frequency data very well, and apparent resistivities in the conductive area are not low enough.

A 2-D finite-element dipole-dipole resistivity computer pro-

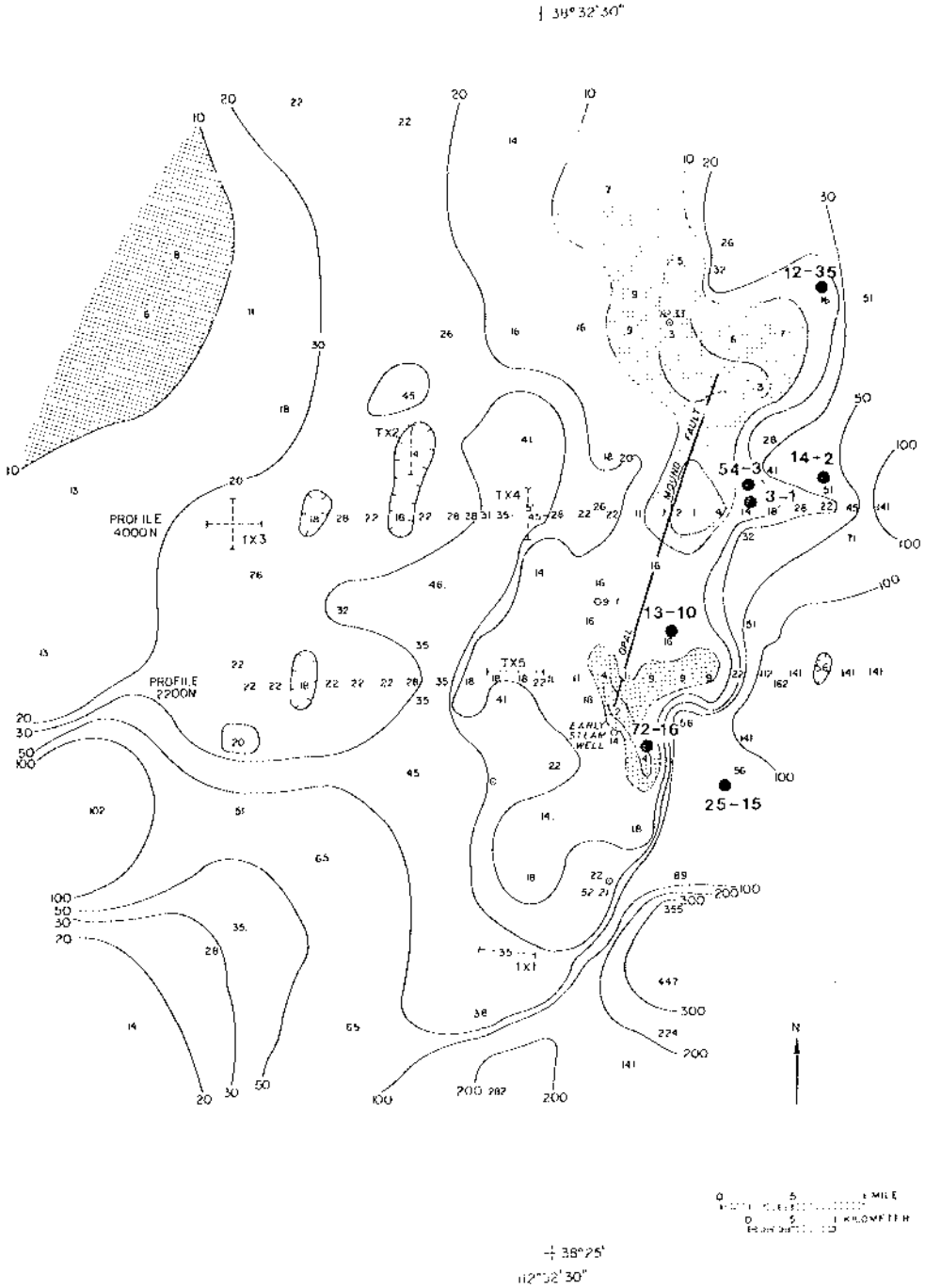

FIG. 11. CSAMT apparent resistivity map of Roosevelt Hot Springs KGRA. Frequency = 98 Hz. Areas less than 10 Ω·m are shaded.

gram (Killpack and Hohmann, 1979) was used to generate resistivity data from the CSAMT model. A comparison of this theoretical data and the resistivity field data is shown in Figure 18.

The dipole-dipole resistivity data in Figure 18 indicate a resistive overburden from CSAMT station 3900 on the west end of the profile. Lack of high-frequency data at stations 2100, 3000, 3300, 3600, and 3900 (Figure 13) along with probable noise at the high-frequency reading at station 2700 contribute to CSAMT's inability to detect this feature. The CSAMT model (Figure 15) was constructed to fit the field data, and therefore it does not show a resistive overburden.

One large disagreement between the resistivity and CSAMT interpretations is the depth to the conductive unit from stations 2400 to 3600 (Figure 15). This depth is modeled 300 m deep by resistivity and 150 m deep by CSAMT. Joint modeling of 300-m and 1-km dipole-dipole data by Ward and Sill (1976) on this line also indicated a resistive-to-conductive interface at 300 m. The similarity between TM and TE mode CSAMT data in this region (see Figures 13 and 14) suggests that 1-D inversion results should be meaningful. We inverted data from stations 2400 through 3600 to determine the depth to this conductive zone.

Inversion results indicate that the 150-m interface modeled by CSAMT is a shallow limit, and the 300-m interface modeled by resistivity is too deep. An inversion of Schlumberger resistivity sounding data (Tripp et al, 1978) obtained just west of station 3300 indicates a resistive-to-conductive interface at about 119 m with a range of 73 to 196 m. When EM sounding data (10.5 Hz to 86 kHz) in the same position were inverted (Tripp et al, 1978),

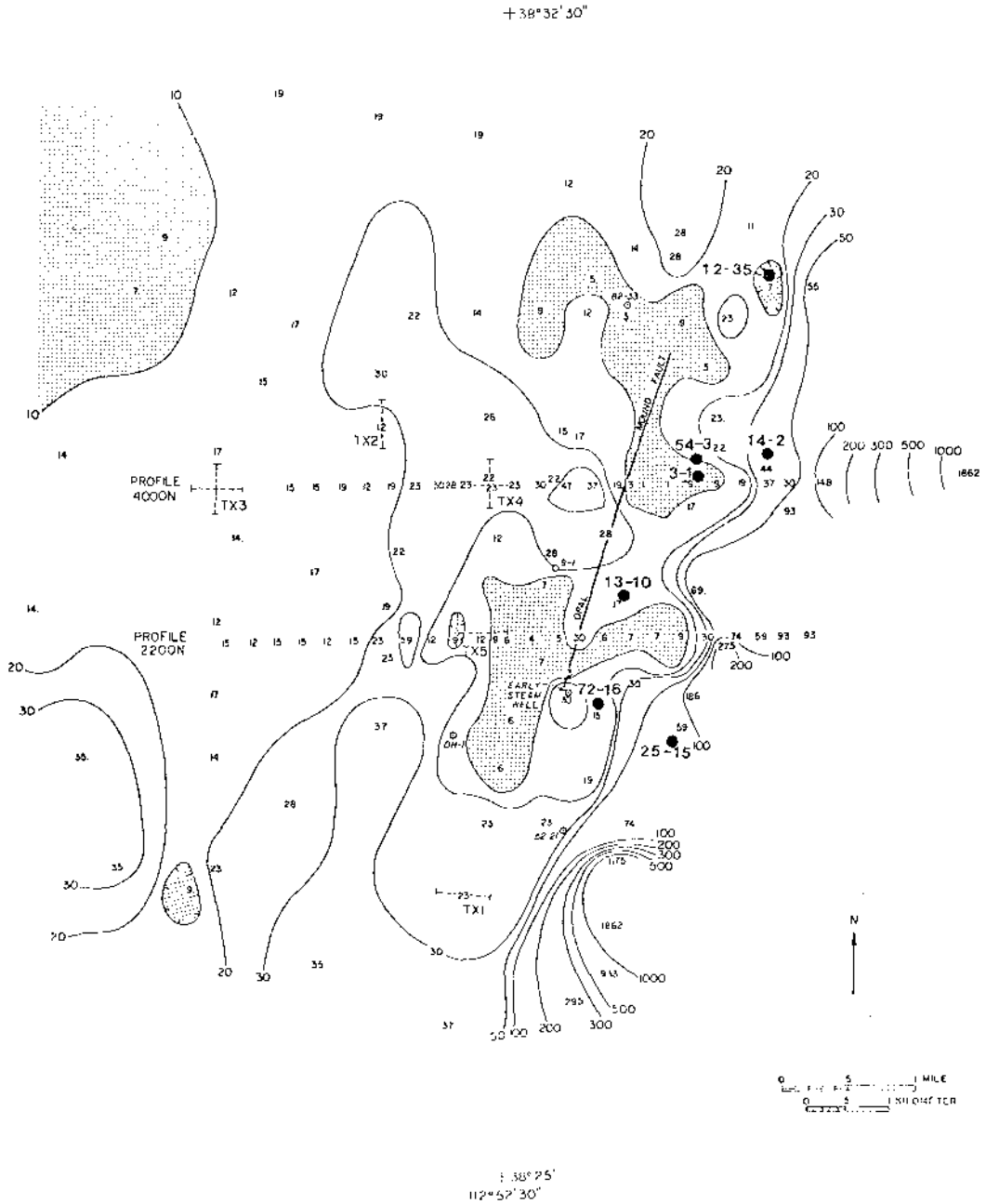

FIG. 12. CSAMT apparent resistivity map of Roosevelt Hot Springs KGRA. Frequency = 32 Hz. Areas less than 10 Ω-m are shaded.

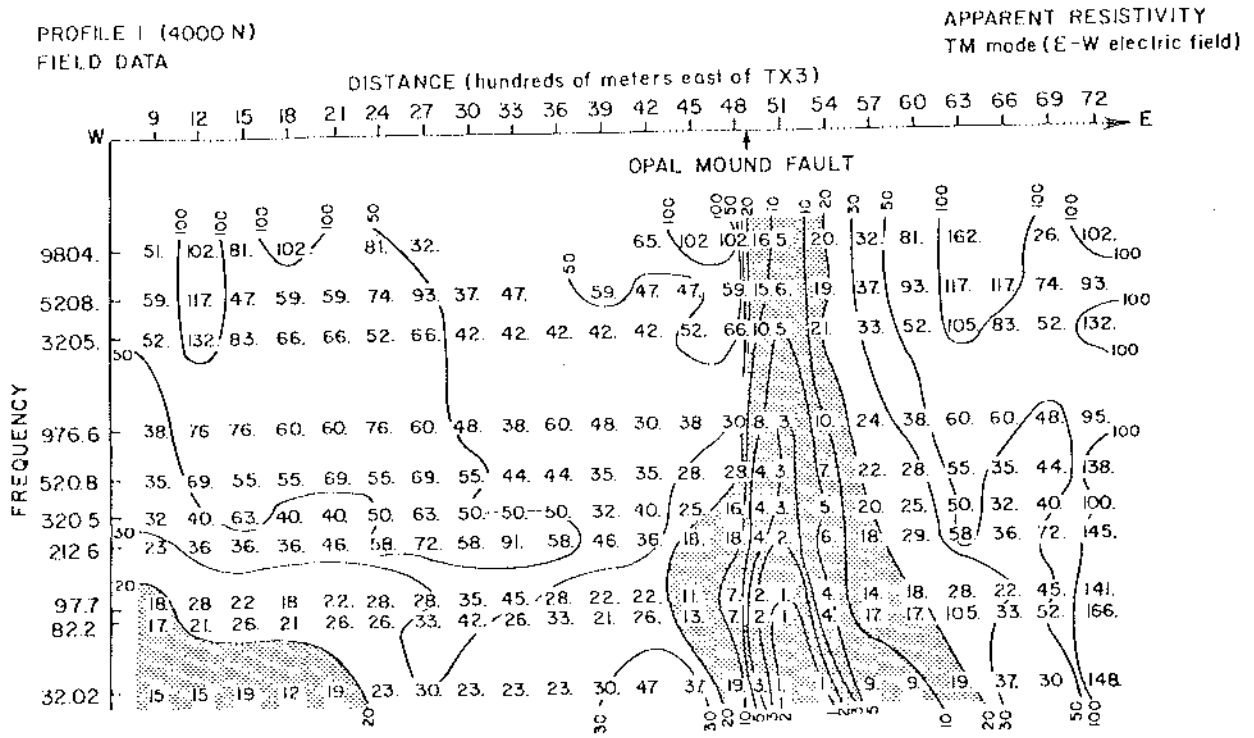

FIG. 13. TM mode field data pseudo-section from profile 1 (4000 N). Apparent resistivity less than 20 Ω-m is shaded.

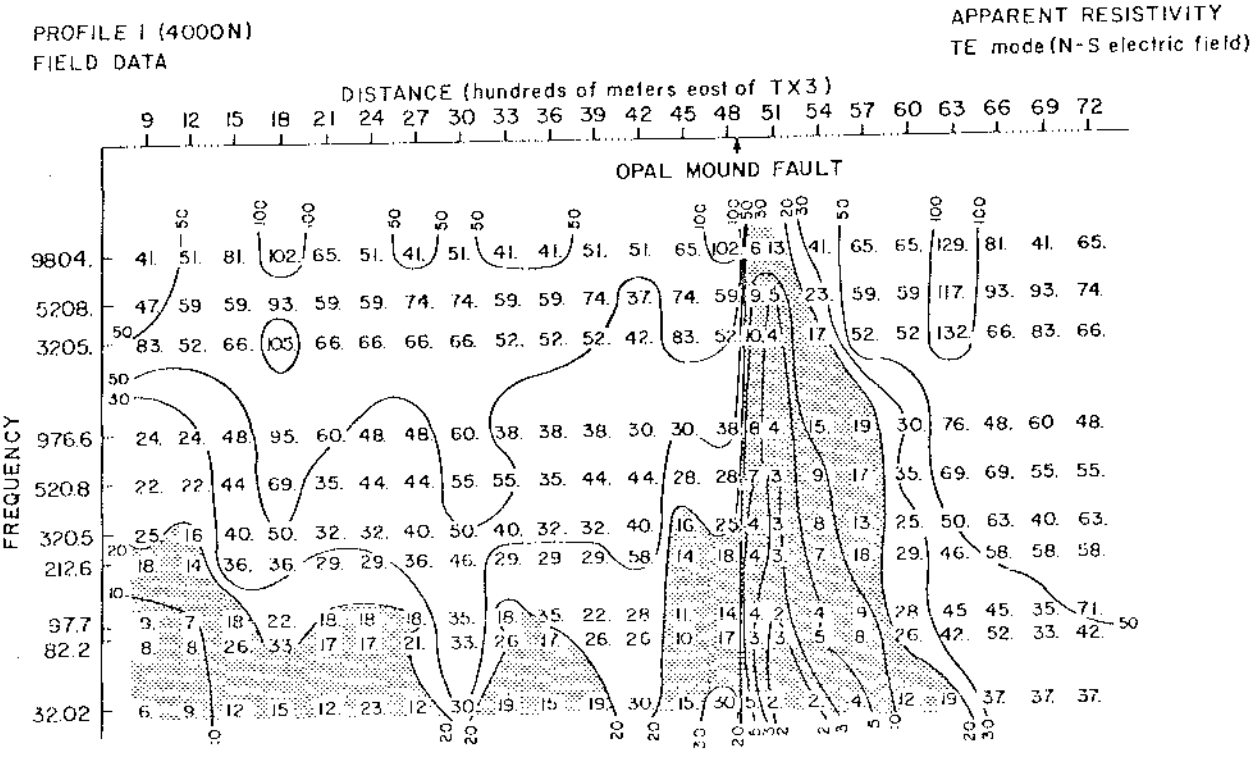

FIG. 14. TE mode field data pseudo-section from profile 1 (4000 N). Apparent resistivity less than 20 Ω m is shaded.

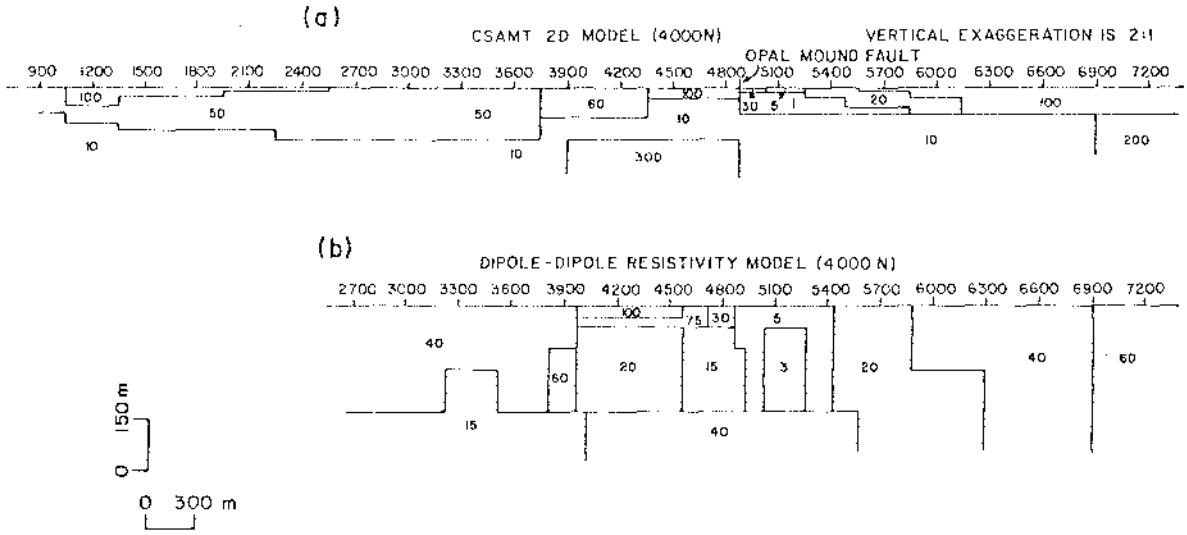

FIG. 15. (a) Two-dimensional CSAMT and (b) dipole-dipole resistivity (based on 100 m and 300 m dipoles) interpretations of profile 1 (4000 N).

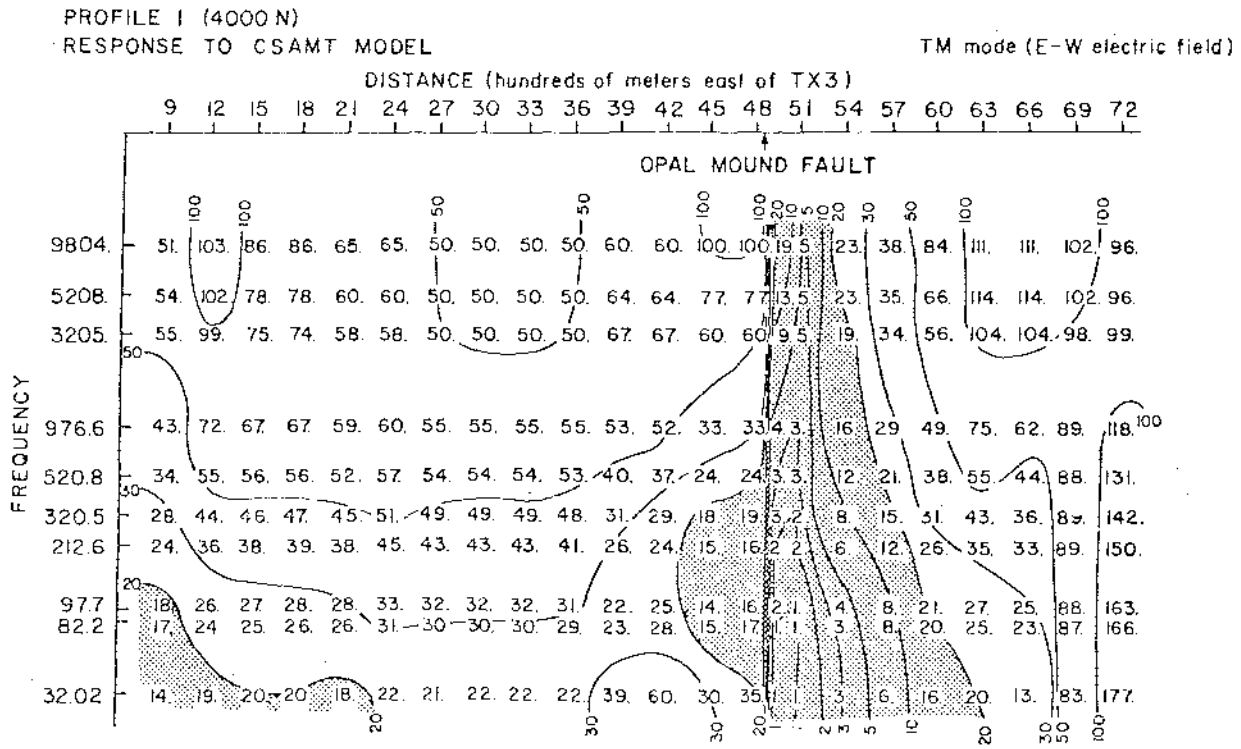

FIG. 16. Theoretical TM mode pseudo-section calculated from 2-D CSAMT model of profile 1 (4000 N). Apparent resistivity less than 20 Ω-m is shaded. Compare with field data in Figure 13.

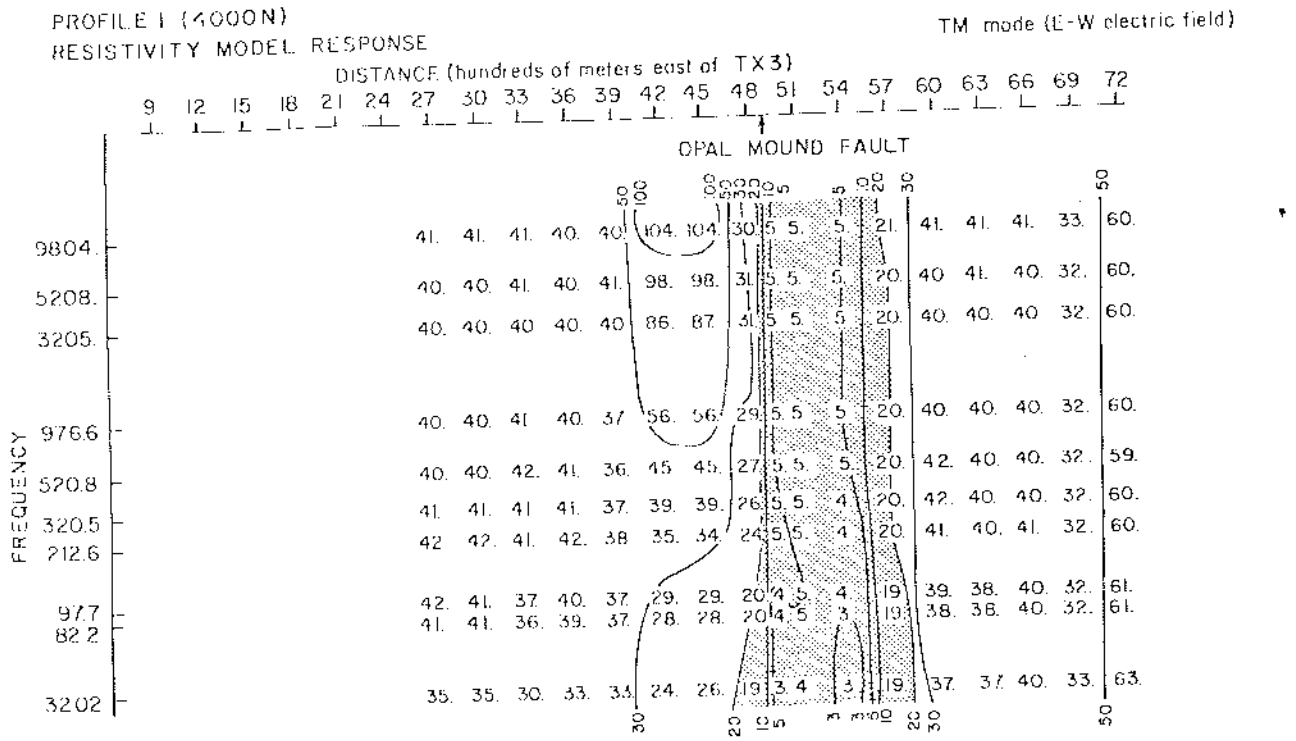

FIG. 17. Theoretical TM mode pseudo-section calculated from 2-D dipole-dipole resistivity model of profile 1 (4000 N). Apparent resistivity less than 20 Ω·m is shaded. Compare with field data in Figure 13.

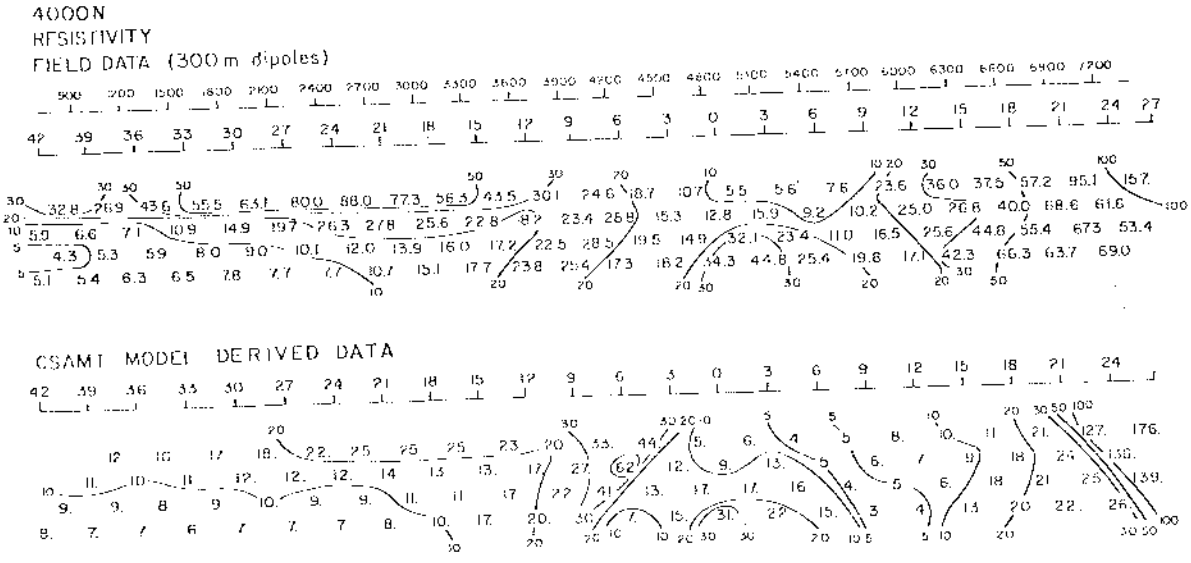

FIG. 18. Dipole-dipole (a = 300 m) resistivity field data compared with theoretical dipole-dipole data calculated from the CSAMT model of profile 1 (4000 N).

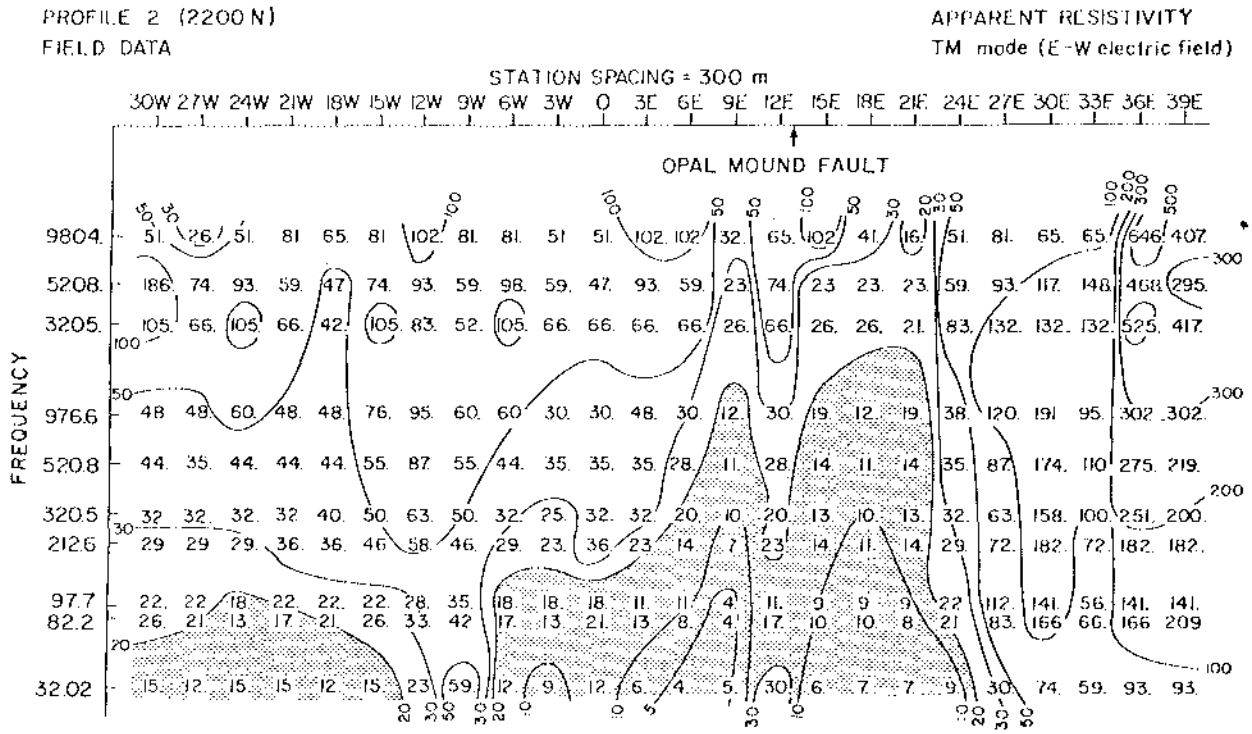

FIG. 19. Field data pseudo-section from profile 2 (2200 N). Apparent resistivity less than 20 Ω-m is shaded.

15 m of 119 Ω-m overburden underlain by 55 Ω-m material was interpreted. The EM sounding, although unable to penetrate to the resistive-conductive interface, gave a check on the resistivity of the upper layer. Based on this information, the upper layer resistivity for the CSAMT inversion was constrained at 50 Ω-m, eliminating high parameter correlations.

A 300 Ω-m resistive body corresponding to bedrock at depth is the main feature in the CSAMT section from 3900 to 4800. This body is modeled 150 m deep, but the depth is not well resolved. It is not shown in the interpretation of the dipole-dipole data (Figure 15b). The evidence for this resistive block occurs at the two lowest frequencies at stations 4200 and 4500, and the lowest frequency at stations 3900 and 4800. Two-dimensional Schlumberger modeling 500 m to the south of this line (Tripp et al, 1978) delineated a 300 Ω-m block at a similar depth. The joint 300-m and 1-km dipole-dipole model (Ward and Sill, 1976) indicates a 300 Ω-m substratum 600 m deep from station 3900 eastward.

The ability to resolve a narrow resistive structure at depth is related to the depth of exploration. The CSAMT technique, using the skin depth criterion, has a depth of exploration in 10 Ω m material of 280 m (at 32 Hz). However, sensitivity tests indicate that the depth of exploration is less than a skin depth with our instrumentation due to apparent resistivities being repeatable only within a factor of 1.26. The dipole-dipole technique at $n = 4$ has depths of exploration of about 120, 360, and 1200 m for 100 m, 300 m, and 1 km dipoles, respectively (Roy and Apparao, 1971) for a plane interface. For tabular vertical structures, depths of exploration are less than for a plane interface. However, the 300-m dipole-dipole data should include information about the 300 Ω-m block. However, probably due to nonuniqueness of resistivity modeling, this block was not modeled (see Figure 15b).

Gravity modeling on this line (Crebs, 1976) shows bedrock 70 m deep below station 4800 increasing to about 140 m just west of station 4200. By adjusting the density contrast to a more reasonable value, Tripp (1977) suggested that the depth could compare quite reasonably with the 150 m modeled here. This resistive body is most likely unaltered Precambrian gneiss bedrock.

A thermal gradient hole was drilled a short distance from station 4800, intersecting the water table at 35 m. This depth coincides with the CSAMT model interface between 100 and 10 Ω-m material at 40 m depth.

Just east of station 4800 there is a sharp surface lateral resistivity contrast corresponding to the Opal Mound fault mapped by resistivity, heat flow, and geology. Inversion of EM sounding data shows 19 m of 24 Ω-m material underlain by 3.4 Ω-m material in this position (Tripp et al, 1978). This agrees well with the CSAMT model of 15 m of 30 Ω-m material underlain by 1 Ω-m material. The bottom of the 1 Ω-m block and the east edge of the 300 Ω-m block (see Figure 15) are not resolved because the near-surface region is so conductive that it is impossible to "see through" it at these frequencies. The eastern end of the 1 Ω-m unit is modeled as a staircase structure which implies a shallow, eastward dipping altered zone east of the Opal Mound fault.

A sensitivity study helped to explain the lack of fit in the theoretical dipole-dipole pseudo-section (Figure 18) from station 5100 eastward. An AMT 1-D study to simulate the resistivity section beneath station 5100 indicated that it was not possible to

determine the resistivity of anything below a 15 m layer of 5 Ω-m material overlying 60 m of 1 Ω m material, even though a skin depth in 1 Ω-m material at 32 Hz is 89 m. When the errors in data measurement are considered, the thickness of the 1 Ω-m layer could be decreased to about 40 m and still shield information from below. Therefore, the exploration depth in this case is less than 0.6 skin depths.

A similar study simulating the resistivity section beneath station 5400 indicated no information could be derived about material below a 20 Ω-m layer 30 m thick overlying a 1 Ω-m layer 45 m thick. The depth of exploration is therefore less than .8 skin depths.

Based on the sensitivity tests, a model similar to the CSAMT model in Figure 15 was constructed which fit the 300 m dipole-dipole data out to station 6000. The modified model included thinning the 1 Ω-m layer and inserting 40 Ω-m material beneath it under stations 5100 to 5700. Lack of fit east of station 6000 is likely due to the fact that the area is not 2 D because of faulting parallel to the traverse 500 m to the north.

Profile 2

Profile 2 is an east-west traverse along resistivity line 2200N and is located 1800 m south of profile 1 (see Figure 9). The data are plotted in pseudo section form in Figure 19. Five stations in the center of the line (6W, 3W, 0, 3E, and 6E) were obtained using transmitter TX4, and the rest were taken by working off both ends of transmitter TX5 [an east-west, 2000 ft (609.6 m) bipole]. Hence the data shown in Figure 19 are for the TM mode (i.e., east-west electric field).

Low-frequency data at station 9W erroneously indicate a resistive body at depth, because the station was too close to the transmitter. For a 50 Ω m earth at 32 Hz, the distance from the center of the transmitter (at 0) to 9W is only 1.4 skin depths. Thus the low-frequency data at station 9W were not modeled.

As in the previous profile, 1-D MT inversion was used at individual stations to construct an initial 2-D model. Trial-and-error, 2-D, TM mode MT modeling improved the data fit, resulting in the CSAMT interpretation model in Figure 20a. The data fit is illustrated by comparing the theoretical data in Figure 21 with the field data in Figure 19. Figure 20b shows a 2-D dipole-dipole resistivity model of the same line (Ross et al, 1981) for comparison. Again, a theoretical AMT pseudo section derived from the resistivity model (not shown) does not fit the field data very well.

The resistivity and CSAMT models are similar. At 6W on the profile, the resistive-to-conductive interface depth is 90 m in the resistivity model compared to 70 m in the CSAMT model, although the resistivity values are somewhat different.

A gravity interpretation of this profile (Crebs, 1976) shows a 230 m wide bedrock horst below station 12E buried 30 m deep. The Opal Mound fault lies on the east flank of this horst. We modeled a resistive block 300 m wide, 155 m from the surface in the same position. A value of 300 Ω-m was chosen for the resistivity to coincide with a similar bedrock structure on profile 1. The model derived from dipole-dipole resistivity data indicates a similar resistive structure at station 1200E: a 100 Ω-m block 150 m wide and 300 m deep. This resistive structure, an extension of the one from profile 1, is most likely unaltered Precambrian gneiss bedrock.

Another similarity between the CSAMT and resistivity models is a contact between 24E and 27E. Resistivity increases to the east corresponding to the unaltered but weathered granitic Mineral Mountains pluton.

CONCLUSIONS

Controlled source AMT appears to be an effective method for rapidly mapping the near-surface expression of a geothermal system. CSAMT resistivity mapping at Roosevelt Hot Springs

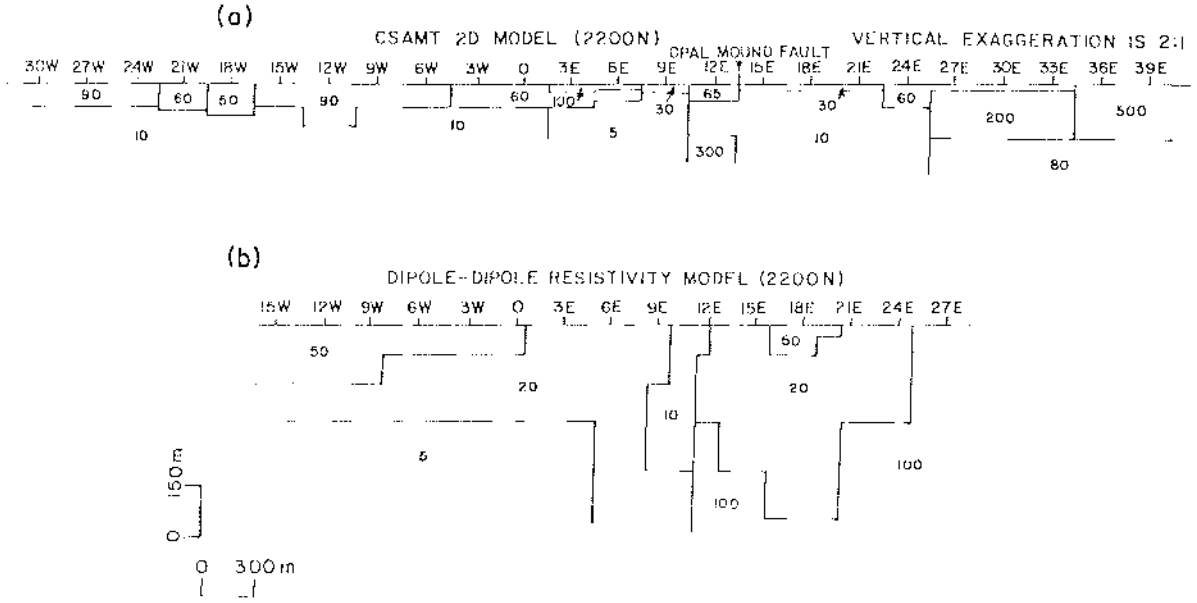

FIG. 20. (a) Two dimensional CSAMT and (b) dipole-dipole resistivity (based on 100 m and 300 m dipoles) interpretations of profile 2 (2200 N).

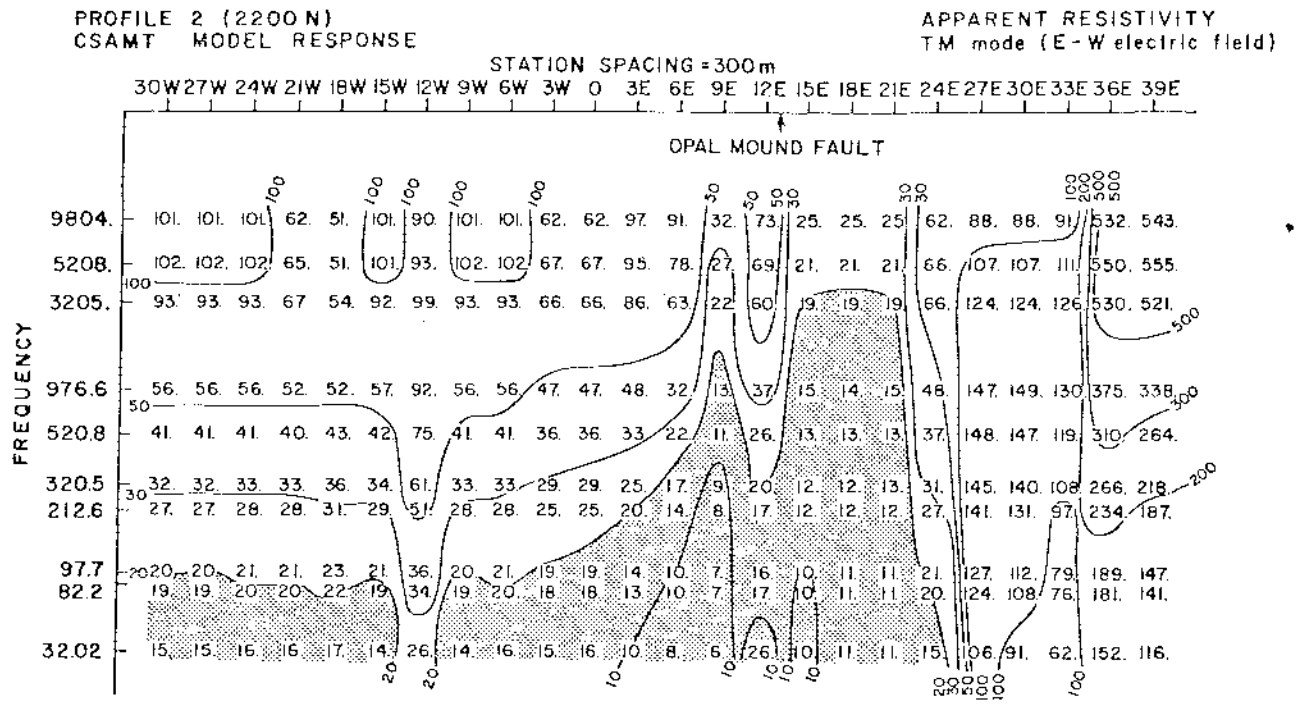

FIG. 21. Theoretical pseudo-section calculated from 2-D CSAMT interpretation of profile 2 (2200 N). Apparent resistivity less than 20 Ω-m is shaded. Compare with field data in Figure 19.

KGRA delineates the same low-resistivity zones as those shown on a first separation 300-m dipole-dipole resistivity map. However, the CSAMT data were collected more rapidly because stations were not constrained to lines, long wires were not necessary, and only two transmitter sites were required. While no cost study was made, we believe that CSAMT would be cost comparable, or more likely, more cost effective than dipole-dipole resistivity mapping in a geothermal environment.

Profiling with CSAMT using 10 frequencies and subsequent 2-D TM-mode modeling produced interpretations consistent with other geophysical and geologic evidence. Two-dimensional modeling of profile 1, supported by gravity data, indicates a resistive structure at depth probably corresponding to unaltered bedrock beneath stations 3900 to 4800. A shallow, eastward-dipping conductive zone, probably altered alluvium due to brine leakage from the Opal Mound fault, is indicated from stations 5100 to 5700. Profile 2 indicates a resistive structure at depth below station 12E in the same position as a bedrock horst modeled by gravity. Alteration and/or brine leakage is indicated on both east and west sides of the Opal Mound fault along profile 2.

A good initial guess for a 2D CSAMT model can be obtained by stitching together 1-D inversions for all stations. This appears to be an advantage over dipole dipole 2-D modeling where an initial guess is not as easily obtained.

The ambiguity of electrode effects inherent in the dipole-dipole technique is not present in CSAMT since the receiver samples only the ground nearby which is independent of the transmitter. If the transmitter is far enough removed, the source field is approximately a plane wave yielding measurements which are source independent.

Skin depth considerations suggest that CSAMT mapped the electrical resistivity to 300 m depth in conductive areas. However, modeling and sensitivity tests confirmed the findings of Strangway et al (1973) that the technique has difficulty detecting structure beneath conductive overburden. Depth of exploration, given the accuracy of our measurements, was found to be considerably less than a skin depth in conductive areas.

ACKNOWLEDGMENTS

We wish to thank Kennecott Minerals Co. for providing the receiver used in the field work. Technical advice and assistance were gratefully received from W. SanFilipo, W. Petrick, P. Wannamaker, and J. Stodt. We also wish to thank S. H. Ward, C. M. Swift, Y. Shoham, and W. D. Stanley for critically reviewing the manuscript. This work was supported under DOE contract number DE-AC07-80ID12079.

REFERENCES

Crebs, T. L., 1976, Gravity and ground magnetic surveys of the central Mineral Mountains, Utah: M. S. thesis, Univ. of Utah.

Glenn, W. E., and Hulen, J. B., 1979, Interpretation of well log data from four drill holes at Roosevelt Hot Springs KGRA: Univ. of Utah Research Inst., Earth Science Lab. Rep. 28, DOE/DGE contract EG-78-C-07-1701.

Goldstein, M. A., and Strangway, D. W., 1975, Audio frequency magnetotellurics with a grounded electric dipole source: Geophysics, v. 40, p. 669–683.

Hohmann, G. W., 1975, Three-dimensional induced polarization and electromagnetic modeling: Geophysics, v. 40, p. 309–324.

Hoover, D. B., Frischknecht, F. C., and Tippens, C., 1976, Audio-magnetotelluric soundings as a reconnaissance exploration technique in Long Valley, Calif.: J. Geophys. Res., v. 81, p. 801–809.

Hoover, D. B., and Long, C. L., 1976, Audio-magnetotelluric methods in reconnaissance geothermal exploration: Proc. 2nd U.N. Symp. Dev. Geothermal Resources, p. 1059–1064.

Hoover, D. B., Long, C. L., and Senterfit, R. M., 1978, Some results

from audiomagnetotelluric investigations in geothermal areas: Geophysics, v. 43, p. 1501–1514.
Kan, T., and Clay, C. S., 1979, Hybrid-ray approximation in electromagnetic sounding: Geophysics, v. 44, p. 1846–1861.
Killpack, T. J., and Hohmann, G. W., 1979, Interactive dipole-dipole resistivity and IP modeling of arbitrary two-dimensional structures (IP2D users guide and documentation): Univ. of Utah Research Inst., Earth Science Lab. Rep. 15, DOE/DGE contract EG-78-C-07-1701.
Long, C. L., and Kaufman, H. E., 1980, Reconnaissance geophysics of a known geothermal resource area, Weiser, Idaho, and Vale, Oregon: Geophysics, v. 45, p. 312–322.
Ross, H. P., Nielson, D. L., Smith, C., Glenn, W. E., and Moore, J. N., 1981, An integrated case study of the Roosevelt Hot Springs Geothermal System, Utah: Submitted to AAPG Bull.
Roy, A., and Apparao, A., 1971, Depth of investigation in direct current methods: Geophysics, v. 36, p. 943–959.
Sandberg, S. K., 1980, Controlled-source audiomagnetotellurics in geothermal exploration: M.S. thesis, Univ. of Utah.
Stodt, J. A., 1978, Documentation of a finite-element program for solution of geophysical problems governed by the inhomogeneous 2-D scalar Helmholtz equation: NSF grant AER-11155, U. of Utah, 66 p.
Strangway, D. W., Swift, C. M., and Holmer, R. C., 1973, The application of audio-frequency magnetotellurics (AMT) to mineral exploration: Geophysics, v. 38, p. 1159–1175.
Ting, S. C., and Hohmann, G. W., 1981, Integral equation modeling of three-dimensional magnetotelluric response: Geophysics, v. 46, p. 182–197.
Tripp, A. C., 1977, Electro-magnetic and Schlumberger resistivity sounding in the Roosevelt Hot Springs known geothermal resource area: M.S. thesis, Univ. of Utah.
Tripp, A. C., Ward S. H., Sill, W. R., Swift, C. M., Jr., and Petrick, W. R., 1978, Electromagnetic and Schlumberger resistivity sounding in the Roosevelt Hot Springs KGRA: Geophysics, v. 43, p. 1450–1469.
Wannamaker, P. E., Ward, S. H., Hohmann, G. W., and Sill, W. R., 1980, Magnetotelluric models of the Roosevelt Hot Springs thermal area, Utah: Univ. of Utah Dept. Geol. and Geophys. rep. DOE/ET/27002-8, 213 p.
Ward, S. H., and Sill, W. R., 1976, Dipole-dipole resistivity surveys, Roosevelt Hot Springs KGRA: NSF final rep., v. 2, grant GI-43741, Univ. of Utah, 29 p.
Ward, S. H., Parry, W. T., Nash, W. P., Sill, W. R., Cook, K. L., Smith, R. B., Chapman, D. S., Brown, F. H., Whelan, J. A., and Bowman, J. R., 1978, A summary of the geology, geochemistry, and geophysics of the Roosevelt Hot Springs thermal area, Utah: Geophysics, v. 43, p. 1515–1542.